The Effects of Chain Length and Thermal Denaturation on Helix-Forming Peptides: A Mode-Specific Analysis Using 2D FT-IR

D. K. Graff,[†] B. Pastrana-Rios,[‡] S. Yu. Venyaminov,[†] and F. G. Prendergast*,[†]

Contribution from the Department of Pharmacology, The Mayo Clinic and Foundation, 1417 Guggenheim, 200 First Street SW, Rochester, Minnesota 55905, and University of Puerto Rico, Mayaguez Campus, Office M224, Post Street, Mayaguez, Puerto Rico 00681-5000

Received February 18, 1997. Revised Manuscript Received June 5, 1997[⊗]

Abstract: The major goal of this project was to use FT-IR spectroscopy to monitor the effects of chain length and temperature on small, helix-forming peptides of the general form, Ac-W(EAAAR)$_n$A-NH$_2$, where $n = 1$, 3, 5, and 7, in aqueous solutions. FT-IR spectra were collected in D_2O as a function of temperature in the range of −4 to 95 °C. The spectral range of interest, 1500−1725 cm^{-1}, contains the amide-I′ band of the fully-exchanged H → D peptide bond. Even in these simple peptides, the amide-I′ region of the IR spectra is complex and congested, composed of features derived from the conformation of the peptide backbone and from the contributions of amino acid side chains. Unambiguous resolution of peak positions and intensities is thus extremely difficult, particularly when assessing subtle differences between two data sets. Two-dimensional correlation analysis (Noda, I. *J. Am. Chem. Soc.* **1989,** *111,* 8116. Noda, I. *Applied Spectrosc.* **1990,** *44,* 550) was used to guide and verify the results of the peak-fitting procedure and thereby facilitate physical interpretation of the temperature-dependent spectra. The results of the two-dimensional analysis and fitting procedure show that the spectral bands, particularly those of the amide-I′ band, exhibit significant frequency shifts and bandwidth and intensity changes as a function of temperature and chain length. For the amide-I′ modes arising from the helical and random conformations of the peptide bond, the normalization of peak intensities to units of molar absorptivity is discussed in terms of different models. Two different molar absorptivity calculations are presented, the first using the length-dependence of α-helical frequencies as predicted by perturbation theory, and the second assuming a more rigorous two-state transition. The results from each are discussed in terms of the effects of chain length on α-helix stabilization and in terms of a mechanism of helix unfolding.

Introduction

Model peptides have been studied spectroscopically in an attempt to understand the principles governing secondary structure formation and stability of peptides and proteins in solution. The experimental and spectroscopic tools available for probing the structures of such systems include circular dichroism (CD), Raman scattering, infrared absorption, fluorescence, NMR, EPR, and X-ray diffraction. Each of these techniques provides a unique but unavoidably limited perspective, although, with sufficient effort, NMR methods can provide complete physical descriptions if problems inherent in the use of high sample concentrations do not arise and if size limitations are not exceeded. The best overall experimental approach clearly is to apply a variety of spectroscopic methods to a problem, thereby to establish as many correlations as possible between all of the measurable signals and the secondary structural features which give rise to them. The implicit expectation of such studies is that an understanding of the forces and mechanisms which determine the secondary structural features in simplified model peptides will afford fundamental principles leading to increasingly more accurate interpretations of the secondary structures of more complex peptides and proteins.

The α-helical properties of short peptides have been most extensively studied.[1−6] Marqusee and Baldwin[1a] were the first to examine the helix-forming properties of short Ala-based peptides. Using circular dichroism (CD) spectroscopy, they quantified the helix-stabilizing effect of variably spaced Glu$^-$/Lys$^+$ salt bridges. Huyghues-Despointes et al.[1b] later employed NMR to measure the positional dependence and energetics of Gln-Asp side-chain interactions in the stabilization of related helical peptides. Stellwagen et al.[2a] used circular dichroism to monitor the structural effects of various X-residue substitutions in the helix-forming peptide, Ac-(EAAAK)(EAXAK)(EAAAK)A-NH$_2$, and to probe the effects of pH and ionic strength on helix stability. These peptides were related to those from an earlier study[2b] in which an E/R rather than an E/K peptide pair (and various others) was shown to provide the most favorable

* To whom correspondence should be addressed.
† The Mayo Clinic and Foundation.
‡ University of Puerto Rico.
⊗ Abstract published in *Advance ACS Abstracts,* October 15, 1997.

(1) (a) Marqusee, S.; Baldwin, R. L. *Proc. Natl. Acad. Sci. U.S.A.* **1987,** *84,* 8898. (b) Huyghues-Despointes, B. M. P.; Klingler, T. M.; Baldwin, R. L. *Biochemistry* **1995**, *34(41),* 13267.
(2) (a) Park, S. H.; Shalongo, W.; Stellwagen, E. *Biochemistry* **1993,** *32,* 12901. (b) Merutka, G.; Stellwagen, E. *Biochemistry* **1991,** *30,* 1591. (c) Shalongo, W.; Stellwagen, E. *Protein Science* **1995,** *4,* 1161.
(3) Shalongo, W.; Dugad, L.; Stellwagen, E. *J. Am. Chem. Soc.* **1994,** *116,* 2500.
(4) (a) Zimm, B. H.; Bragg, J. K. *J. Chem. Phys.* **1959,** *31,* 526. (b) Lifson, S.; Roig, A. *J. Chem. Phys*. **1961**, *34,* 1963. (c) Stapely, B. J.; Rohl, C. A.; Doig, A. J. *J. Protein Science* **1995,** *4,* 2383. (d) Scholtz, J. M.; Baldwin, R. L. *Annu. Rev. Biophys. Biomol. Struct.* **1992,** *21,* 95. (e) Vasquez, M.; Scheraga, H. A. *Biopolymers* **1988,** *27,* 41. (f) Padmanabhan, S.; York, E. J.; Stewart, J. M.; Baldwin, R. L. *J. Mol. Biol.* **1996,** *257,* 726.
(5) (a) Yuan, P.; Fisher, P. J.; Prendergast, F. G.; Kemple, M. D. *Biophys. J.*, **1996**, *70,* 2223. (b) Kemple, M. D.; Buckley, P.; Yuan, P.; Prendergast, F. G. *Biochemistry* **1997**, *36,* 1678−1688.
(6) (a) Fiori, W. R.; Miick, S. M.; Millhauser, G. L. *Biochemistry* **1993,** *32,* 11957. (b) Miick, S. M.; Martinez, G. V.; Fiori, W. R.; Todd, A. P.; Millhauser, G. L. *Nature* **1992,** *359,* 653. (c) Fiori, W. R., Millhauser, G. L. *Biopolymers* **1995**, *37,* 243. (d) Miick, S. M.; Casteel, K. M.; Millhauser, G. L. *Biochemistry* **1993**, *32,* 8014.

S0002-7863(97)00512-X CCC: $14.00

ionic interactions of the side chains, stabilizing the helical conformation.[2c] To further understand helix formation and stability, these workers then investigated[3] the helix-forming peptide, Ac-W(EAAAR)$_3$A-NH$_2$, using ^{13}C NMR and CD to monitor the effects of pH, ionic strength, and temperature on helical content. They inferred a two-state helix/coil transition, with the helical structure stabilized by intrachain hydrogen bonding and charge−charge interactions. The ^{13}C NMR measurements distinguished individual residue positions and thus gave insight into the mechanism of thermal denaturation of the helix. Further, with increasing temperature, charge−charge side-chain interactions were observed to rupture first, followed by the dissociation of backbone (intrachain) hydrogen bonds initially at the ends of the helix and moving towards the middle. These ideas are generally consistent with the models for helix-to-coil transformation of Zimm and Bragg[4a] and Lifson and Roig.[4b] Subsequent authors have added to this basic model, including effects such as capping of the helical ends and directional salt bridge formation between side-chain residues.[4c−f] In the model, residues are characterized by their tendency to initiate and propagate helix conformation. The *i*th residue, internal to the chain, is stabilized by hydrogen bonding to the $i + 4$ and $i - 4$ peptides; residues on the ends, being not bidirectionally stabilized by hydrogen bonding, exist in a less uniform conformation and are thus the first to respond to thermal agitation.

Our research group, employing ^{13}C NMR to study the helical structures of melittin, has observed the extent of such "end effects" to be largely a function of peptide environment.[5] In a further examination of chain length and "end effects" on helix stability and unfolding, Millhauser et al. studied[6] model peptides similar to those discussed above. In these studies, ESR was used to probe the structure of a series of 16-mer helix-forming peptides, doubly-labeled with nitroxide moieties and exploiting the distance dependence of spin-spin interactions. From their results, these authors deduced that peptides of this length and shorter appear to adopt a substantial percentage of 3_{10} helix conformation; for longer chains, the occurrence of 3_{10} conformation is usually limited to the last two to three residues on the C-terminus.

Infrared absorption, and particularly Fourier transform infrared spectroscopy (FT-IR), has also proven to be a valuable tool for probing the secondary structure of biopolymers in the steady state.[7,8] Additionally, transient infrared absorption has been used elegantly to monitor, in real time, the kinetics of the peptide folding/unfolding process.[9] The amide-I′ and II′ vibrations (denoted with a prime′ for samples studied in D_2O solution), intrinsic to the peptide bond, have been shown to be highly sensitive to the secondary structure of the peptide. However, the interpretation of FT-IR spectra of biopolymers is often difficult because they are almost invariably congested with many peaks arising from both the peptide backbone and the amino acid side chains. Various methods of spectral analysis have been employed in attempts to solve this problem, including second-derivative and Fourier deconvolution.[10]

A new method of spectral deconvolution has been introduced recently. Noda's two-dimensional method of analysis[11] has been shown to be particularly well-suited for the deconvolution of FT-IR spectra subjected to some perturbation. This procedure calculates correlation intensities of all the various frequency components in the system as their peak intensities change with respect to an applied perturbation. Spectral deconvolution is facilitated when these correlation intensities are plotted as contour maps on a double frequency axis. Convoluted peaks which are perturbed differently will show different correlations with other peaks and thus be "drawn out" differently on the second frequency axis.

The work in this paper represents the initial component of an extended study underway in our laboratory in which NMR, FT-IR, and CD spectroscopy[7a] are being used to probe the secondary structural properties of peptides. We describe the use of FT-IR spectroscopy to probe the effects of chain length in a series[3] of helix-forming peptides, Ac-W(EAAAR)$_n$ A-NH$_2$, with $n = 1$, 3, 5, and 7. FT-IR spectra for each of the four peptides in D_2O solution were collected over a large temperature range (approximately −4 to 95 °C) to monitor the temperature induced changes in secondary structure. The peptides have been simultaneously characterized in H_2O by use of circular dichroism (CD) measurements. We used the unique properties of the 2D analysis for the deconvolution of the temperature dependent FT-IR data. We propose an application of this technique for situations in which the most straightforward rules of interpretation[11,13] cannot be utilized.

Materials and Methods

Peptides were synthesized in the Mayo Peptide Synthesis Facility by use of FMOC (9-fluorenyl-methoxycarbonyl) strategy. Peptides were purified by reverse phase HPLC. Peptide purity and molecular weight, assessed by time of flight mass spectrometry, were found to be within 1 *m/z* range of the expected values. The peptides were further purified by extensive dialyses against 0.1 N HCl to remove TFA, which absorbs in the infrared range of interest. For spectral measurements, the pH was adjusted to 7.0, and samples were dialyzed a second time against 10 mM phosphate and 10 mM NaCl at pH 7.0, and for studies with D_2O as a solvent, peptide samples were lyophilized several times out of D_2O to effect complete proton to deuterium exchange. FT-IR measurements were conducted with solutions of peptides at ∼20 mg/mL.

A custom-made cell and shuttle system were used for data accumulation on a Bio-RAD FTS-40 FT-IR spectrophotometer. The shuttle is equipped with a thermostated brass block which holds both sample and reference cells. Use of an enclosed shuttle system minimizes error due to differences in sample and reference cell temperature, atmospheric water vapor content or atmospheric CO_2 concentration, and baseline drift. The reference cell contains phosphate buffer at the same concentration as the sample. This procedure[7b] employs two polished CaF_2 cells, with a reference and sample thickness equal 40.2 and 41.1 microns, respectively. The longer pathlength of the sample cell compensates for the dilution of the solvent by the presence of the protein, such that the absorbance of the solvent (D_2O) will be essentially the same in both cells. Compensation was also made for absorptions due to different isotopic ratios of H/D in the sample and reference by varying the exposure time of the reference buffer to atmospheric water vapor (H_2O). Temperature was varied by use of an RTE-111 Neslab circulating bath; a thermal probe was used to measure

(7) (a) Venyaminov, S. Yu.; Prendergast, F. G. Work in progress. (b) Venyaminov, S. Yu.; Prendergast, F. G. *Anal. Biochem.* **1997,** 248, 234.

(8) (a) Martinez, G.; Millhauser, G. *J. Struct. Biol.* **1995,** *114*, 23. (b) Venyaminov, S. Yu.; Kalnin, N. N. *Biopolymers* **1990**, 30, 1259. (c) Tanfani, F.; Kochan, Z.; Swierczynski, J.; Zydowo, M. M.; Bertoli, E. *Biopolymers* **1995,** *36*, 569.

(9) Williams, S.; Causgrove, T. P.; Gilmanshin, R.; Fang, K. S.; Callender, R. H.; Woodruff, W. H.; Dyer, R. B. *Biochemistry* **1996**, *35*, 691.

(10) (a) Susi, H.; Byler, D. M. *Methods Enzymol.* **1986,** *130*, 290. (b) Surewicz, W. K.; Mantsch, H. H. *Biochem. Biophys. Acta* **1988,** *952*, 115. (c) Moffatt, D. J.; Mantsch, H. H. *Methods Enzymol.* **1992,** *210*, 192.

(11) (a) Noda, I. *Applied Spectrosc.* **1990,** *44*, 550. (b) Noda, I. *J. Am. Chem. Soc.* **1989,** *111*, 8116. (c) Noda, I.; Dowrey, A. E.; Marcott, C. *Applied Spectrosc.* **1993,** *47*, 1317.

(12) (a) Venyaminov, S. Yu.; Gogia, Z. V. *Eur. J. Biochem.* **1982,** *126*, 299. (b) Venyaminov, S. Yu.; Yang, J. T. *Circular Dichroism and the Analysis of Biomolecules*; Fasman, G. D., Ed.; Plenum Press: New York, 1996. (c) Mihaly, E. *J. Chem. Eng. Data* **1968,** *13(2)*, 179.

(13) (a) Noda, I. *Applied Spectrosc.* **1993,** *47*, 1329. (b) Ekgasit, S.; Ishida, H. *Applied Spectrosc.* **1995,** *49*, 1243.

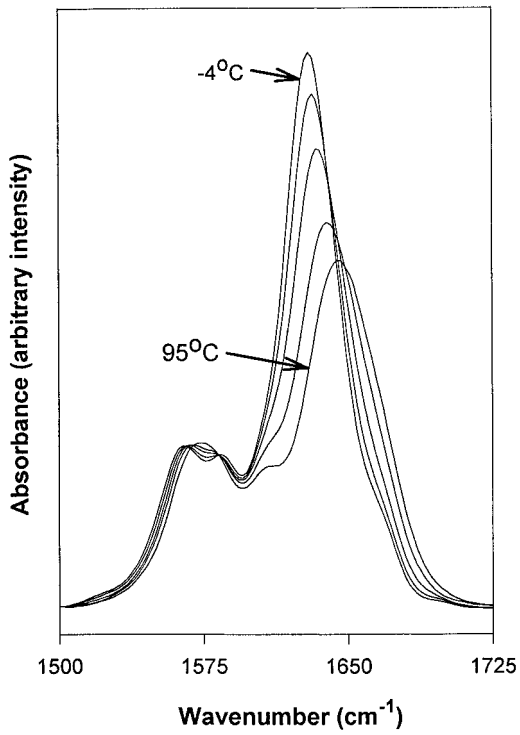

Figure 1. Typical temperature-dependent FT-IR spectra of Ac-W(EAAAR)$_7$A-NH$_2$ in D_2O in the spectral range of 1500−1725 cm^{-1}. Spectra shown are for temperatures of −4, 15, 30, 45, and 95 °C.

the temperature (values ±0.5 °C). Typically, 512 scans were co-added and apodized with a triangular function to yield a resolution of 2 cm^{-1}. In the 2D analysis and spectral fitting procedure, a two-point determination of baseline was made at 1500 and 1725 cm^{-1}, where sample absorption was minimal.

Temperature-dependent spectra were collected sequentially with the sample held in the sealed and equilibrated compartment of the FT-IR spectrophotometer. The procedure involved the collection of 16 spectra for each peptide through the temperature range, −4 to 95 °C. This number of spectra was chosen so that fast Fourier algorithms could be used in the computation of cross-correlation intensities. For two of the peptides, $n = 3$ and $n = 5$, spectra were collected at only 12 and 15 different temperature increments; again, for the correlation calculations, to keep the total number of spectra at 16, four and one of the spectra in the temperature-dependent sequence of $n = 3$ and $n = 5$, respectively, were repeated. This was done for both the calculated and fitted data and did not therefore adversely effect the 2D analysis. Temperature-dependent FT-IR spectra collected for the $n = 7$ peptide in D_2O solution are displayed in Figure 1. Spectral variations with temperature were observed to be fully reversible.

Frequencies of the peak maxima of the amide I′ region for the four peptides are plotted as a function of temperature in Figure 2. The broad spectral band in this region contains contributions from both the α-helix and random coil configurations, and the frequency shifts observed as a function of temperature are largely a result of the transition from one secondary structural form to the other. Peak deconvolution and analysis procedures were performed in seeking a physically-relevant interpretation of the experimental data.

CD measurements were made on a Jasco J-710 spectropolarimeter. Concentration of samples was determined using a Cary 2200 UV−visible spectrophotometer to measure Trp absorption at 280 nm using an extinction coefficient of 5579 M^{-1} cm^{-1}. Corrections were made for sample turbidity. This procedure and that for the instrumental calibration were as given previously.[12] At 0 °C, the α-helical content of each sample was determined to be 14 ± 4% for $n = 1$, 73 ± 7% for $n = 3$, 83 ± 10% for $n = 5$, and 90 ± 8% for $n = 7$. At 90 °C, the α-helical content was 6 ± 5% for $n = 1$, 12 ± 2% for $n = 3$, 12 ± 2% for $n = 5$, and 17 ± 4% for $n = 7$. This structural interpretation of CD data was based on three different methods of calculation[12c] with a reference set containing native proteins rather than peptides.

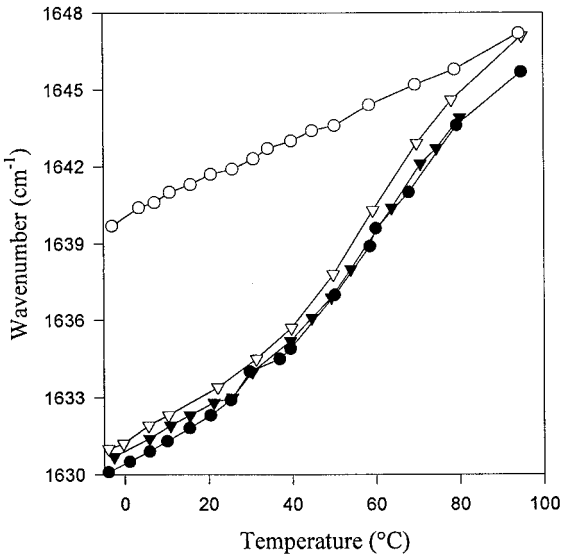

Figure 2. Peak maxima of amide I′ bands from −4 to 95 °C, of Ac-W(EAAAR)$_n$A-NH$_2$ in D_2O (○ denotes the $n = 1$ peptide, ▽ is the $n = 3$ peptide, ▼ is the $n = 5$ peptide, and ● is the $n = 7$ peptide). Data points are connected to guide the eye.

The two-dimensional correlation analyses were performed using MathCad 6.0 (MathSoft, Inc.) software, as were the preliminary data simulations. Curve-fitting was done with the GRAMS 3.01 package (Galactic Industries Corporation).

Data Analysis

Theory and Background. Two-dimensional correlation spectroscopy was proposed by Noda[11] for the analysis of infrared data. Noda's work has since been extended for general applicability[13] to any spectral signals which vary as a function of an applied perturbation. The analysis involves Fourier transformation of the experimental spectra and the construction of a correlation matrix such that intensity arises at the intersection of spectral frequencies which respond very similarly or very differently to the perturbation. The real and imaginary intensities in the correlation matrix are viewed as contour plots, bringing the perturbation response of the system graphically to the forefront for analysis. With high sensitivity, 2D analysis highlights the dynamic correlations between different spectral components. In complex systems where the spectra are congested, the analytical technique is inherently useful in resolving the overlapped spectral components.[14] 2D analysis has thus found wide application, particularly for various spectroscopic studies of polymeric systems.[15] The computation of 2D spectra is briefly summarized below. More detailed theoretical discussions can be found elsewhere.[11,13]

The experimental data are represented by matrix $F_{v,t}$, spectral intensities which vary as a function of spectral frequency, v, and perturbation, t. The dynamic spectral information is retained as $D_{v,t}$ using

$$D_{v,t} = F_{v,i} - A'_v, \text{ for } i = 1 \text{ to } t \qquad (1a)$$

(14) (a) Sonoyama, M.; Shoda, K.; Katagiri, G.; Ishida, H. *Applied Spectrosc.* **1996**, *50*, 377. (b) Noda, I.; Liu, Y.; Ozaki, Y. *J. Phys. Chem.* **1996,** *100*, 8665. (c) Noda, I.; Liu, Y.; Ozaki, Y. *J. Phys. Chem.* **1996,** *100*, 8674.

(15) (a) Nakano, T.; Shimada, S.; Saitoh, R.; Noda, I. *Applied Spectrosc.* **1993,** *47*, 1337. (b) Ebihara, K.; Hiroaki, T.; Noda, I. *Applied Spectrosc.* **1993,** *47*, 1343. (c) Gregoriou, V. G.; Chao, J. L.; Toriumi, H.; Palmer, R. *Chem. Phys. Lett.* **1991,** *179*, 491.

where A'_v is the average of all spectra measured

$$A'_{v,t} = \frac{\sum_i^t F_{v,i}}{t} \tag{1b}$$

and t is the total number of spectra measured.

A one-dimensional Fourier transform, row-wise on matrix $D_{v,t}$, results in a complex matrix:

$$C_{v,f} = FFT(D_{v,t}) \tag{2}$$

The cross-correlation of this matrix is the cross-product of itself with the transpose of its complex conjugate. The cross-correlation intensity matrix, $I_{v1,v2}$, has real and imaginary parts which represent the synchronous correlation, $\Theta_{v1,v2}$, and the asynchronous correlation, $\Psi_{v1,v2}$, respectively,

$$C_{v,f} \times \overline{C^T_{v,f}} = \mathrm{Re}[I_{v1,v2}] + \mathrm{Im}[I_{v1,v2}]$$
$$= \Theta_{v1,v2} + \Psi_{v1,v2} \tag{3}$$

The contents of these matrices, plotted separately on axes of $v1$ and $v2$, comprise the synchronous and asynchronous cross-correlation intensities of the chemical system with the perturbation. Peak positions in the 2D plots are represented by a pair of frequency coordinates. Spectral contours and intensities are typically interpreted using a set of rules, found elsewhere.[11a,13b] The rules assess positive/negative intensities of a peak in both the synchronous and the asynchronous spectrum to determine the correlation and phase relationship of the various frequency responses.

2D Analysis of FT-IR Spectra of Peptides. In this study, it was anticipated that IR signals derived from various components of the peptide secondary structure would respond differently to temperature changes. The 2D analysis would then provide a means by which the multiple infrared components could be resolved, identified, and compared for each peptide. The above cross-correlation calculations were carried out on the experimental temperature-dependent spectra of each of the peptides, $n = 1$, 3, 5, and 7, and the results for $n = 1$ and $n = 7$ are shown in Figures 4A, 4B, 5A, and 5B, respectively. In proceeding with the 2D analysis, we found it was not possible to interpret the cross-correlation plots using the prescribed rules.

Noda's analysis (and set of rules) is based on the implicit assumption that spectral *intensities* are sensitive to the perturbation, while spectral *frequencies* are not. Frequency changes appear to invalidate application of Noda's rules of analysis by causing corresponding intensity maxima to occur at different frequency positions on the synchronous versus the asynchronous plots. Simple spectral simulations indicated that many of the contours observed in our data could be most-simply reproduced by allowing peak positions to move along with the peak intensities. Other authors have attributed similar features in 2D contour plots to frequency shifts in studies of polymeric amides.[16]

Based on these findings, we approached the use of 2D analysis in a new way. Because direct application of Noda's rules was not possible, we modeled the experimental spectra using a minimum set of spectral peaks and a least-squares minimization routine to obtain the best possible fits. Comparison of the experimental and simulated 2D correlation plots was then used as a further criterion in the fitting procedure to test the validity of the fitting model used. Application of the 2D technique in this way proved useful in determining the *minimal* model, i.e., that with the fewest number of parameters which adequately described the temperature-dependent changes in the spectra. Obviously, a larger number of peaks and parameters could be used to fit the data giving lower least-square errors and better fits to the 2D correlation plots; however, the validity and usefulness of such an over-parameterized model is questionable, its parameters being difficult or impossible to interpret. In addition to determining a model with the minimal number of peaks, reproduction of the experimental 2D contours served as a useful criterion for determining the best bandshapes for use in the fitting procedure.

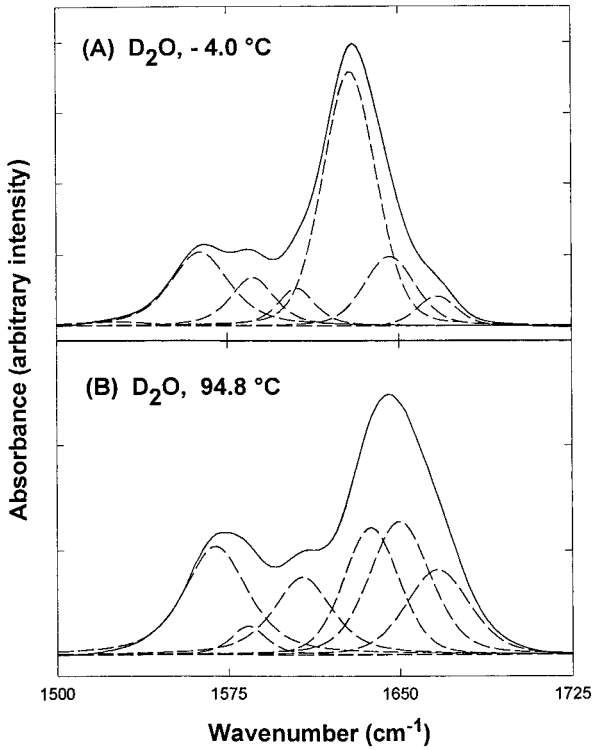

Figure 3. Spectral fitting results for (A) −4 °C and (B) 95 °C spectra of Ac-W(EAAAR)$_7$A-NH$_2$ in D_2O, experimental spectrum (—), and fitted subbands (- - -). Peak compositions, in terms of Gaussian and Lorentzian fractions, were determined from the literature,[17] as were the initial placements of peak frequencies. Final fits determined by least-squares analysis (see text).

Models and Spectral Fitting. Many attempts were made to fit the spectra using sets of different numbers of peaks with stationary frequencies, i.e., peaks that did not change frequency with temperature. If peak frequencies were held fixed, a large number of peaks (>10) had to be included in order to reproduce the experimental 2D plots. Data simulations indicated that the most prominent contours in the experimental 2D data could be reproduced if peak frequencies in that region were allowed to have even a small temperature-dependent shift. By defining peak frequency as a variable parameter in our curve-fitting, the number of peaks required to obtain good least-square fits and to reproduce the 2D contours was significantly reduced. Thus the temperature-dependence of spectral frequencies was an important factor in the determination of a "minimum model," i.e., the minimum number of peaks providing a satisfactory fit to the data. After many fitting attempts, peak widths were constrained to a maximum value of 40 cm^{-1}; this was primarily to keep the positions well-defined and the parameters changing consistently from one temperature to the next.

(16) (a) Singhal, A.; Fina, L. J. *Appl. Spectrosc.* **1995,** *49(8),* 1073. (b) Sonoyama, M.; Kunihiro, S.; Katagiri, G.; Ishinda, H. *Appl. Spectrosc.* **1996,** *50(3),* 377.

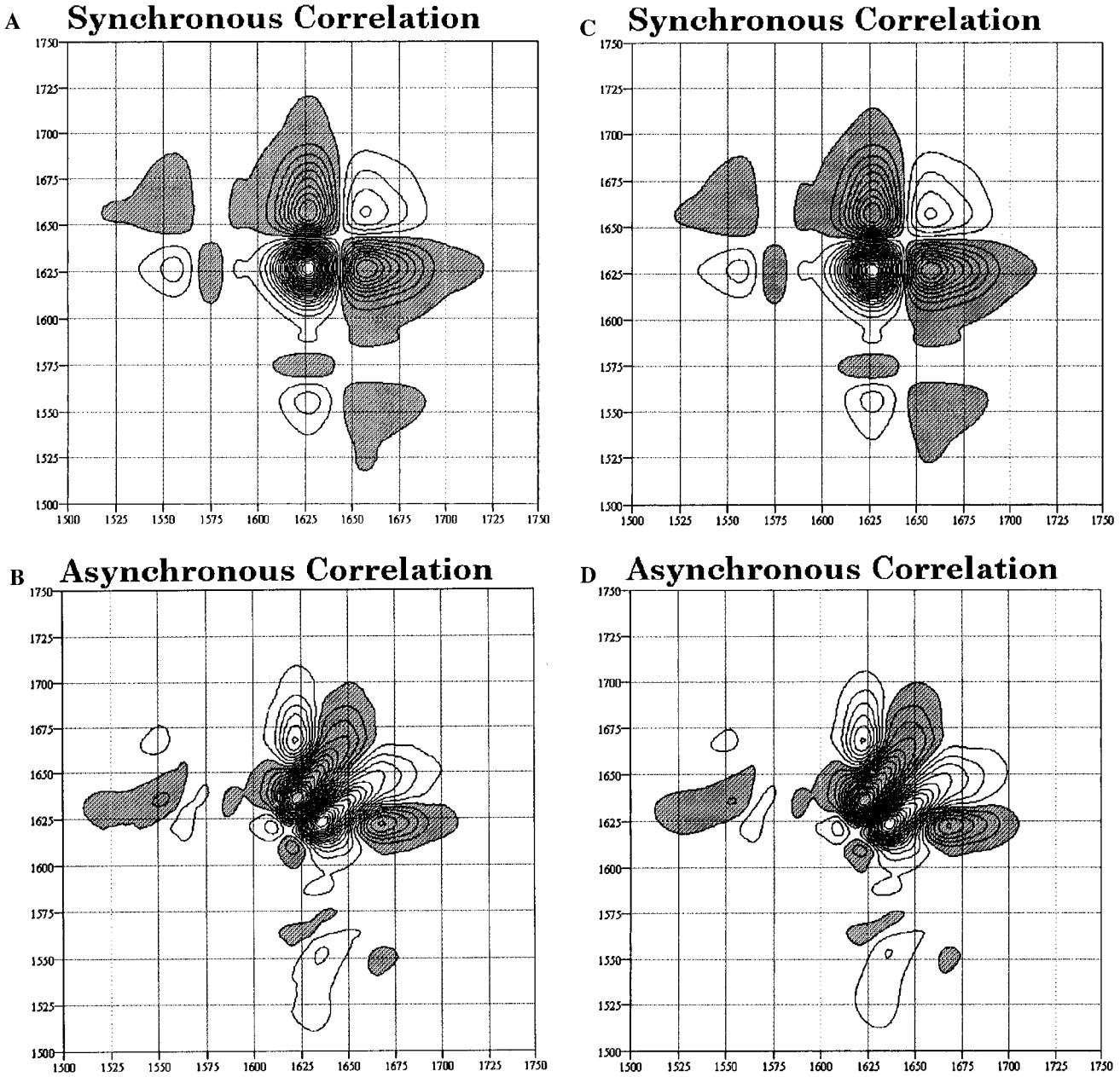

Figure 4. Synchronous and asynchronous 2D correlation plots for the temperature-dependent spectra of Ac-W(EAAAR)$_7$A-NH$_2$ in D_2O: (A and B) experimental and (C and D) simulated (peak fitted, see text). Lighter regions represent positive going contours, darker regions are negative.

In summary, the frequencies, widths (to 40 cm^{-1}), and heights of the above six peaks were free parameters allowed to vary in order to achieve the lowest least-squared value for the fit of each spectrum at each temperature. The peaks from our final "minimal model" coincided very well with the physical model based on previous studies[17] of IR signals of various peptides and amino acid derivatives in D_2O. The approximate frequencies (and the assignments) of the expected peaks for our peptides included 1636 ± 2 cm^{-1} (amide I′ of α helix),[17a] 1672 ± 3 cm^{-1} and 1648 ± 2 cm^{-1} (amide I′ of random coil),[17c] 1608 cm^{-1} and 1586 cm^{-1} (asymmetric and symmetric stretches, respectively, of the arginine side chain),[17b] and 1567 cm^{-1} (asymmetric stretch of the glutamic acid side chain).[17b] In addition, a peak was included with a fixed frequency at 1527 cm^{-1} for all peptides and another at 1695 cm^{-1} in the case of the $n = 1$ peptide. These latter two peaks were of extremely low intensity, but their inclusion in the fitting procedure greatly improved the χ-square values obtained and provided the means by which, for each of the peptides, low- and high-frequency features in the 2D correlation plots could be reproduced. We believe these peaks compensated for small deviations in the baseline, and no attempt was made to assign them to particular functional groups in the peptide systems.

The final parameter set, in accordance with previous studies,[17] used the percent Gaussian component for each peak as follows: 1636 cm^{-1} (80%), 1672 cm^{-1} and 1648 cm^{-1} (70%), 1608 cm^{-1} and 1586 cm^{-1} (40%), 1567 cm^{-1} (40%), 1527 cm^{-1} and 1695 cm^{-1} (50%), with the remainder in each case being Lorentzian. Various fitting procedures were performed using different percentages of Gaussian and Lorentzian bandshapes. We determined that these percentages could be varied 10−20% without inducing a significant change in the results. However, the use of purely Gaussian bandshapes required that further peaks be introduced in order to obtain similar least-squares minima and to reproduce the 2D contour plots. Purely Lorent-

(17) (a) Chirgadze, Yu. N.; Brazhnikov, E. V. *Biopolymers* **1974,** *13,* 1701. (b) Chirgadze, Yu. N.; Fedorov, O. V.; Trushina, N. P. *Biopolymers* **1975,** *14,* 679. (c) Chirgadze, Yu. N.; Shestopalov, B. V.; Venyaminov, S. Yu. *Biopolymers* **1973,** *12,* 1337.

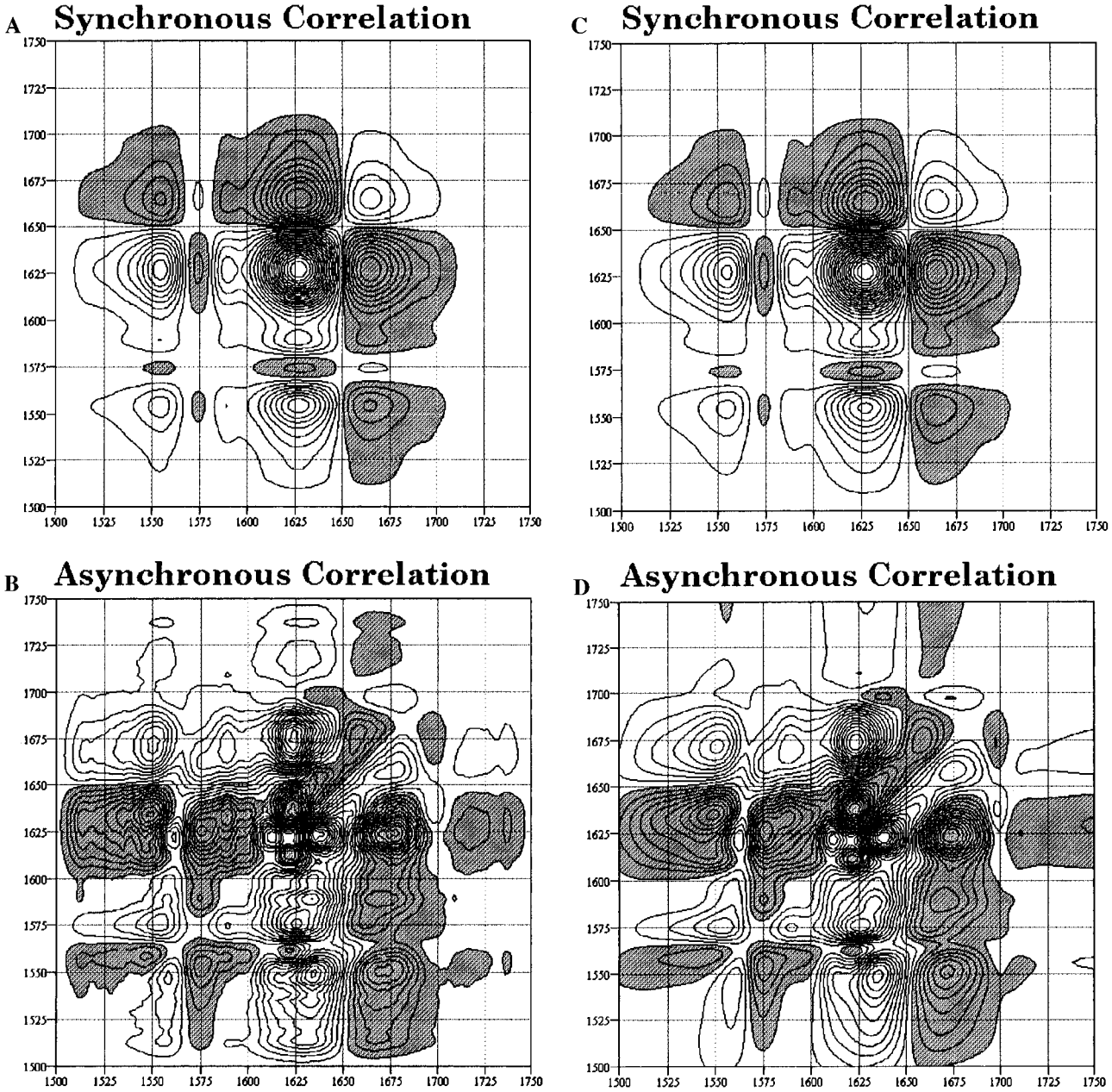

Figure 5. Synchronous and asynchronous 2D correlation plots for the temperature-dependent spectra of Ac-W(EAAAR)$_1$A-NH$_2$ in D_2O: (A and B) experimental and (C and D) simulated (peak fitted, see text). Lighter regions represent positive going contours, darker regions are negative.

zian peaks, even including additional peaks, could not satisfactorily reproduce the low- and high-frequency regions of the 2D plots. These latter two models, with purely Gaussian or Lorentzian peaks, were explored but not used.

Our fitting methodology involved a sequential fitting of spectra from one end of the temperature range to the other as follows. A set of initial frequencies and peak shapes, as discussed above, were used with "by-eye" first guess of intensity values, to fit the lowest (or highest) temperature spectrum. Parameters giving rise to the least-squares fit of this spectrum were then used as the input parameters for fitting the spectrum at the next higher (or lower) temperature. In this way, consistent sets of continuously changing parameters were unambiguously and objectively obtained. In an attempt to treat the data impartially, many models with differing numbers of peaks were initially chosen and the least-squares spectral-fitting procedure carried through, after which, the 2D analysis of the experimental and simulated data was used to select one model over another. Our final fitting results, judged by least-squares minima and satisfactory "by eye" reproductions of the 2D contour plots, gave rise to standard error values between 0.000 45 and 0.000 70 for $n = 7$, 0.000 65 and 0.001 0 for $n = 5$, 0.000 67 and 0.000 91 for $n = 3$, and 0.000 16 and 0.000 36 for $n = 1$, for maximum amide I′ absorbances between 0.21 and 0.74.

Figure 3 shows the high and low temperature spectral-fitting results for the $n = 7$ peptide. These plots are representative of the spectral-fitting results. The 2D correlation analysis was then applied to the best-fit results of the fitting procedure. These plots were judged according to their ability to reproduce the general contour features of the experimental 2D plots. The 2D correlation plots of the best-fit simulation results for the $n = 7$ and $n = 1$ peptides are shown in Figures 4C, 4D, 5C, and 5D, respectively, for comparison with their experimental counterparts, Figures 4A, 4B, 5A, and 5B, respectively.

Results and Discussion

The position of the observed peak maximum for all peptides at −4 °C is in the 1630−1640 cm^{-1} region, Figure 2, consistent with FT-IR studies of other short helical peptides.[8a] At 95 °C,

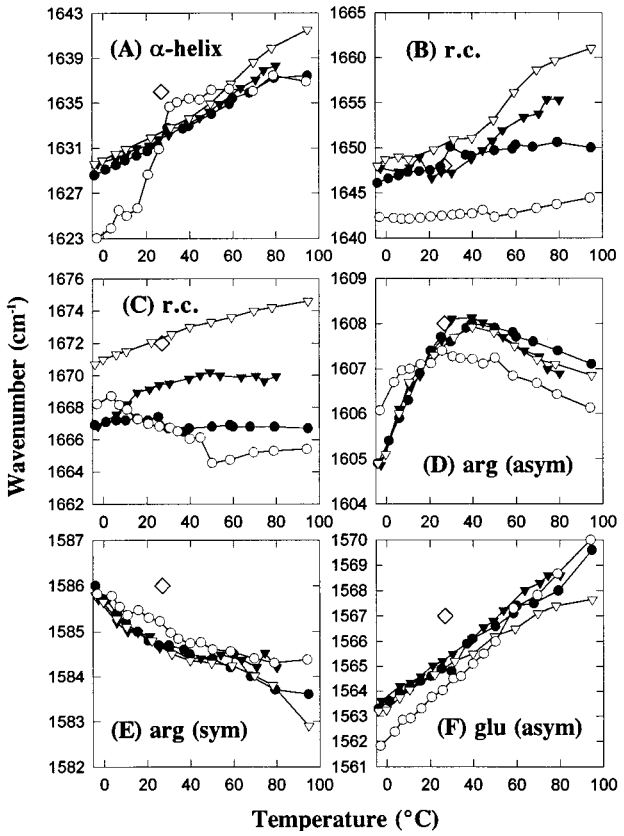

Figure 6. Frequency parameters from the results of spectral fitting all four peptides through the complete temperature range: (A) peak in the 1630 cm^{-1} region, amide I′ of α-helix; (B) peak in the 1650 cm^{-1} region, amide I′ of random coil; (C) peak in the 1670 cm^{-1} region, amide I′ of random coil; (D) peak in the 1607 cm^{-1} region, asymmetric stretch of the Arg residue; (E) peak in the 1585 cm^{-1} region, symmetric stretch of the Arg residue; and (F) peak in the 1565 cm^{-1} region, asymmetric stretch of the Glu residue. (○ denotes the $n = 1$ peptide, ▽ is the $n = 3$ peptide, ▼ is the $n = 5$ peptide, and ● is the $n = 7$ peptide, ◇ denotes the room-temperature point for infinitely long peptides[17a,c] and side-chain residues[17b]). Units are cm^{-1}. In this and the subsequent figures, data points are connected to guide the eye.

for all peptides, the position of the peak is between 1645 and 1647 cm^{-1}. The behavior of the convoluted amide I′ peak is similar for the $n = 3$, 5, and 7 peptides, as opposed to that of the $n = 1$, indicating a "length saturation effect" in the experimental data for $n \geq 3$.

The final results of our spectral fitting and 2D analysis have led us to conclude that, for helical peptides subject to increasing thermal perturbation, the FT-IR spectral components pertaining to secondary structure are best characterized not only by intensity changes but also by frequency and bandwidth changes. The final set of spectral frequencies, molar absorptivities, and bandwidths from the fitting procedure are plotted versus temperature (Figures 6−8, respectively). Included in the display of fitting parameters are the room-temperature values determined from IR studies of long-chain peptides and side-chain derivatives.[17] In general, the $n = 3$, 5, and 7 peptides show similar responses to increasing temperature while those of the $n = 1$ peptide are different. This length saturation point agrees with the results of Merutka et al.[18] and Martinez and Millhauser.[8a]

Frequency Variations with Temperature. In Figure 6A, the helical frequency of the $n = 3$, 5, and 7 peptides increases with increasing temperature. The room-temperature frequency of this helical amide-I′ mode is lower than that usually found in protein α helices (1650 cm^{-1})[19] but in agreement with values[17] for indefinitely long α-helical models (1632 cm^{-1}) and values[8a] found in similar short helix-forming peptide sequences using other deconvolution methods (1632 cm^{-1}). The shift observed for this frequency through the temperature range is significant, 10−11 cm^{-1}, and shows the greatest frequency variation of all the peak positions. The frequency changes for the $n = 3$, 5, and 7 peptides occur with a similar slope, indicating similar responses to the effects of temperature. The $n = 7$ data have a slightly lower *y*-intercept than that of $n = 3$ or $n = 5$. To the extent this difference is outside the error limits of the fitting procedure, this decrease in vibrational energy may indicate a slight stabilization of the helical conformation in longer chains. Perturbation theory,[20] which accounts for the dipolar coupling of oriented amide bonds, predicts a decrease in the frequency of the amide I vibration with increasing chain length and gives a general theoretical basis for the observed effects of temperature (slopes) and chain length (*y*-intercept values) on this mode.

The peak of the $n = 1$ peptide, Figure 6A, is low in intensity (see Figure 7A), with significant magnitude only at low temperatures. Even so, its inclusion is essential in order to reproduce the 2D features in this spectral region of the asynchronous plot. The low frequency of this band and its different response to temperature, when compared to those of the longer peptides, indicates that in the short peptide, this mode is notably different. Due to the low intensity of this peak, the specific structural assignment of this band remains in question, and the error associated with its parameters is assumed to be very large. *A priori*, we must assume that any helical form in such a short peptide represents a highly unstable, fleeting structure in rapid equilibrium with an unordered form.

The frequencies in Figure 6B have been assigned to the amide I′ of the random coil structure. The frequencies increase with increasing temperature, although to a lesser extent than the changes observed for the helical mode in Figure 6A. Analogous to the helical mode, this behavior may be caused by an increased randomization of dipoles due to the thermally-induced increase in local motion. The slopes of the three longer peptides are ordered inversely to their chain lengths, indicating that statistically, the longer-chain random amide-I′ dipoles may be in a more ordered state than are those in shorter peptides. The $n = 1$ random coil frequency, being six to eight wavenumbers lower than those of the longer peptides, may, as with the helical frequency, reflect an entirely different type of dipole distribution or environment than those in the longer chains. Due to the uncertainty of the $n = 1$ data in Figure 6A, it is not clear whether this mode represents the random coil,[17c] belonging in Figure 6B, or better represents a helical contribution[17a] and belongs in Figure 6A. Perturbation theory[20a] predicts a frequency in the 1640 cm^{-1} range for the amide-I′ vibration of an α-helical peptide with this short length, suggesting that the parameters of this mode be included in Figure 6A. However, due to the proximity of the 1640 cm^{-1} mode with the random coil frequencies in the longer chains and due to the presence of the $n = 1$ mode near 1623 cm^{-1}, near to the helical frequencies, we have chosen to plot these modes with those they seem most naturally associated. Comparing the response of the $n = 1$ with those of the $n = 3$, 5, and 7 peptides in Figure 6B, the slope of the $n = 1$ mode is notably more shallow. We assume that the

(18) Merutka, G.; Shalongo, W.; Stellwagen, E. *Biochemistry* **1991,** *30,* 4245.

(19) Stokkum, I. H. M.; Lindsell, H.; Hadden, J. M.; Haris, P. I.; Chapman, D.; Bloemendal, M. *Biochemistry* **1995,** *34,* 10508.

(20) (a) Nevskaya, N. A.; Chirgadze, Yu. N. *Biopolymers* **1976**, *15*, 637. (b) Chirgadze, Yu. N.; Nevskaya, N. A. *Biopolymers* **1976**, *15*, 627. (c) Chirgadze, Yu. N.; Nevskaya, N. A. *Biopolymers* **1976**, *15*, 607.

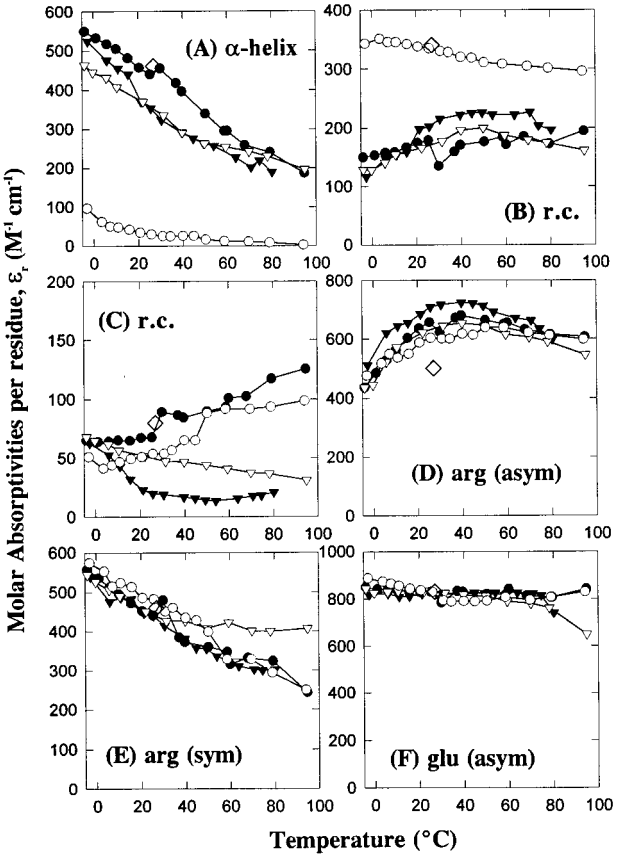

Figure 7. Molar absorptivities calculated *per side-chain residue*, (D), (E), and (F), and *per residue*, (A), (B), and (C), from the peak height results of spectral fitting of all four peptides through the complete temperature range: (A) peak in the 1630 cm^{-1} region, amide I′ of α-helix; (B) peak in the 1650 cm^{-1} region, amide I′ of random coil; (C) peak in the 1670 cm^{-1} region, amide I′ of random coil; (D) peak in the 1607 cm^{-1} region, asymmetric stretch of the Arg residue; (E) peak in the 1585 cm^{-1} region, symmetric stretch of the Arg residue; and (F) peak in the 1565 cm^{-1} region, asymmetric stretch of the Glu residue. (○ denotes the $n = 1$ peptide, ▽ is the $n = 3$ peptide, ▼ is the $n = 5$ peptide, and ● is the $n = 7$ peptide, ◇ denotes the room-temperature point for infinitely long peptides[17a,c] and side-chain residues[17b]). Intensities were normalized using the room-temperature molar absorptivity value of 830 M^{-1} cm^{-1} for the 1567 cm^{-1} mode of the Glu residue.[16b] Molar absorptivities are given in units of M^{-1} cm^{-1}.

parameters for this $n = 1$ mode contain contributions from both helical and random coil configurations.

The frequencies in Figure 6C also pertain to the random coil conformation of the amide-I′ mode.[17c] As in Figure 6B, the frequencies of the $n = 3$, 5, and 7 peptides increase slightly with temperature and possess a magnitude of change inverse to chain length. This amide-I′ band has a low molar absorptivity,[17c] less than 25% the intensity of the random coil band at 1640 cm^{-1}. We believe the parameters of this mode to be effected by slight TFA contamination (see Materials and Methods).

Figure 6D pertains to the asymmetric stretching frequency of the Arg residue side chain, and the shape of its response to temperature is one of the more intriguing results of our analysis. For the $n = 3$, 5, and 7 peptides, an initial rise in frequency, maximizing near 30 °C, is followed by a substantial decrease; for the $n = 1$ peptide, the behavior is similar in shape but with a maximum nearer to 20 °C. The similar response of all the peptides indicates that this mode of the Arg side chain senses temperature changes similarly, regardless of chain length. The response shape suggests the presence of two distinct thermal effects; one which occurs at lower temperatures, and the other of which occurs at higher temperatures. The low-temperature increase is dramatic, similar in scale to the change in the helical frequency seen in Figure 6A. Numerous studies have concluded[2b,3,18] that the Arg and Glu residues serve as charge−charge/hydrogen-bonding partners. The sharp low-temperature increase observed in the 1606 cm^{-1} Arg frequency may indicate that this mode is sensitive to the breaking of these associations which is presumed[3] to be an early occurrence in the thermal disruption of the helical structure. As the bonds break, the ordered structure of these side-chain dipoles is lost, resulting in an increase in the vibrational frequency. Based on this reasoning, one might also predict an incrementing *y*-intercept value for each of the peptides, and similar behavior for the second mode of Arg (1586 cm^{-1}) and the Glu mode; however, these trends are not observed in the data. Above room temperature (>30 °C), changes in the local environment of the side-chain dipole may dominate the IR signal as the helical structure is further dissolved and the polarity of the Arg environment is changed. The thermal response for this mode in the $n = 1$ peptide is similar in shape but maximizes at a lower temperature and possesses only one-third of the magnitude of change.

The behavior of the symmetric stretching frequency of the Arg residue, Figure 6E, is similar for all four peptides. The small thermal and chain length variation suggets a side-chain residue not intimately associated with secondary structure. The decrease of this mode is the smallest of the frequency shifts observed and is similar in magnitude to that observed in the high-temperature region of the mode in Figure 6D. Both of these modes are from the Arg side chain, and it is unclear why their low-temperature behavior would be so different. We cannot exclude the possibility that the different behaviors observed for these two modes are artifactual, arising from limitations of our spectral model.

Figure 6F indicates the behavior of the asymmetric stretching frequency of the carboxylate moiety of the Glu side chain, again similar for all four peptides. Like the helical amide-I′ mode, this frequency shows a significant dependence on temperature, increasing 7−8 cm^{-1} over the temperature range studied. Although notably sensitive to temperature changes, interestingly, the response of this mode is very different from that of either of the modes of Arg, with which it is assumed to associate.

IR Intensity and Bandwidth Variations with Temperature. Molar absorptivity values for the peaks in the n = 1, 3, 5, and 7 peptides are plotted in Figure 7 as a function of temperature. Our normalization of peak intensities for all modes at all temperatures was based on the literature value[17b] of the room-temperature molar absorptivity of the 1567 cm^{-1} Glu vibration in D_2O, 830 M^{-1} cm^{-1}. Our normalization procedure uses this molar value for each peptide and relies on Beer's law:

$$A_{i,p}(T) = \epsilon_{i,p}(T) * C_p * b_{i,p} * l \qquad (4)$$

where $A_{i,p}(T)$ is the peak height (in units of absorbance) determined for the *i*th peak in the *p*th peptide using the curve-fitting procedure, C_p is the molar concentration of the peptide sample, $b_{i,p}$ is the ratio of moles of absorbing dipoles giving rise to the *i*th peak per mole of the *p*th peptide sample, l is the IR cell pathlength, and $\epsilon_{i,p}(T)$ is the temperature-dependent molar absorptivity of the *i*th absorbing dipole in the *p*th peptide.

For each of the four peptides, the value of $C_p * l$ was determined using eq 4, the room-temperature amplitude of the 1567 cm^{-1} Glu peak from the fitted data ($A_{\mathrm{Glu},p}$), the molar absorptivity at that temperature ($\epsilon_{\mathrm{Glu},p}$ = 830 M^{-1} cm^{-1}), and the ratios $b_{\mathrm{Glu},p} = 1$, 3, 5, and 7 (for the $n = 1$, 3, 5, and 7 peptides, respectively). The $C_p * l$ factor was then used to convert the fitted amplitudes of the 1567 cm^{-1} Glu peak to molar

absorptivity values through the full temperature range. For normalization of the two Arg peak heights through the temperature range, the same factor of C_p*l was used along with the appropriate ratios (same as for Glu). Lastly, for normalization of the α-helical and random coil amide-I′ peak heights, consistent with previous work,[17] the C_p*l values were again used, this time with ratios reflecting the total number of residues in each peptide, $b_{\alpha,p} = b_{\text{r.c.,p}} = 7$, 17, 27, and 37. The molar absorptivities for the amide-I′ bands are thus given in units *per residue in the peptide chain*.

Figure 7A shows the change in molar absorptivity of the helical component as a function of temperature. There are slight differences in the behavior of this mode among the $n = 3$, 5, and 7 peptides, including a dip in the $n = 5$ intensity starting near 20 °C and a slight jump in the $n = 7$ intensity near 30 °C. We judge these features to be within the error of the fitting procedure and not indicative of real "discontinuities" in the intensity behavior. The low intensity of the $n = 1$ frequency component in this region precludes any statement regarding its behavior, other than to say that its contribution is extremely small. It is unclear whether these parameters accurately reflect the behavior of the helical mode for the $n = 1$ peptide.

The per residue molar absorptivities for the helical mode can be evaluated for chain length effects, i.e., for differences in average amide-I′ intensities in a short versus a long helix. The room temperature molar absorptivity value for the $n = 7$ peptide coincides very well with the per residue value determined for ideal, indefinitely-long helices,[17] while the absorptivities of the shorter peptides are correspondingly smaller in magnitude. To the extent that a trend exists (outside the limits of error) and decreasing intensities are observed for smaller chain lengths, the similarity of the room-temperature absorptivity for the $n = 7$ peptide to that of the indefinitely-long helices[17] reflects a length saturation point. The study of Merutka et al.[18] concluded that the CD spectra of these peptides showed a length saturation effect at $n = 3$, at which point the spectra became very similar to those of longer, completely-helical peptides. Based on our IR and CD measurements at room temperature,[7a] the length saturation point appears to occur at $n = 7$ or greater.

In a previous study, intensity changes of the helical amide-I′ band were interpreted in terms of helical stability,[17a] a distinct correlation being observed between increases in peak height, decreases in bandwidth, and increases in helix stability. The helical amide-I′ band is composed of a statistical distribution of many oriented dipoles, in slightly different environments and with slightly different dipolar couplings. For a stable and uniform helix, all the dipoles sense a similar environment and possess similar transition energies. When the helix is unstable, a larger statistical ensemble of structures is populated, resulting in inhomogeneous broadening and an increased bandwidth. To the extent that the integrated intensity of the absorptive transition remains constant with conformation changes, increases in bandwidth will be accompanied by corresponding decreases in intensity. Figure 8A shows the full-width at half-maximum changes with temperature for the helical amide I′ band. According to the correlation,[17a] the temperature with the narrowest bandwidth corresponds to that containing the most stable helix. For the $n = 3$, 5, and 7 peptides, the thermal dependence of the width parameter has a minimum which occurs at approximately 28 °C. Below this temperature, the width becomes slightly broader, and above it the width increases considerably. For the $n = 1$ peptide, the bandwidth of this mode reaches an early maximum and does not indicate a particular region of stability. The relationship observed between the molar absorptivity and the bandwidth for this mode in the four peptides cannot simply be explained by the effect of inhomogeneous broadening, although, according to trends observed in a similar study,[8a] inhomogeneous broadening likely plays an important role. More will be said below regarding the interpretation of the absorption intensity of the helix and possible chain length effects.

Figure 7B shows molar absorptivity changes, per residue, associated with the 1648 cm^{-1} amide I′ band and the random coil contributions to secondary structure. For the $n = 3$, 5, and 7 peptides, the intensity response to temperature is what one might predict for a random coil mode as the helix unwinds. The intensity grows with increasing temperature, its most rapid increase occurring near 40 °C. Throughout the temperature range, the $n = 3$, 5, and 7 peptides have similar intensity, while that of the $n = 1$ peptide, at the lower frequency of 1640 cm^{-1} (Figure 6B), is much higher, almost double in magnitude. Interestingly, it is the $n = 1$ peptide which has a molar absorptivity nearly equal to that reported in the study of indefinitely long random coil peptides.[17c] As stated earlier, it is unclear whether the $n = 1$ mode at 1640 cm^{-1} represents the helical or random component of the amide I′ signal or some convolution of the two. The high intensity of this band and its decrease in slope with temperature suggest that it may contain significant helical contributions. However, its position in frequency, and the lack of any other peak in this range assignable to the large component of random coil which must be present in $n = 1$, suggests that this band is best interpreted as arising from the random component. As the predictions of perturbation theory place the helical frequency in this same region, we propose that this band is some convolution of the helix and random coil, showing characteristics of both. We include it in Figure 7B but acknowledge its behavior, and perhaps its identity, as being somewhat different from the other parameters in that plot. We acknowledge also that this band could represent or contain contributions from an alternate helical conformation, such as the 3_{10}-helix, which has been proposed to exist in short, unstable helices.[6,8a]

The thermal increase of inhomogeneous broadening discussed above for the helical amide I′ band might also be expected to occur in that of the random coil, although perhaps to a lesser extent since at low temperatures the structure is already randomized. Figure 8B indicates a thermally-induced increase in the bandwidth for the random component of all four peptides. In addition, the longer peptide chains show a later thermal onset of increased width, indicating that their random component may be more "oriented," with a narrower statistical distribution of conformations at any given temperature. Structurally, the random coil state is a distribution of bond angles subjected to limitations imposed by steric, electrostatic, and other physical properties, and an increase in the thermal energy would fully be expected to alter the statistical distribution of the bond angles, even in an already unordered state. That this broadening effect would be modified by chain length is an interesting observation.

The mode near 1668 cm^{-1} in Figure 7C, also assigned to the random coil, is believed to be effected by slight TFA contamination. The room-temperature molar absorptivities for this amide I′ band are within the range of that reported for the indefinitely-long peptide chains.[17c] Additionally, the intensities of this mode are weak compared to others in this spectral region, from which we conclude that any detrimental effects caused by TFA are localized to the parameters of this single mode.

As with its frequency changes, the molar absorptivity response of the Arg 1606 cm^{-1} mode in Figure 7D is interesting. The intensity response is similar for the $n = 3$, 5, and 7 peptides,

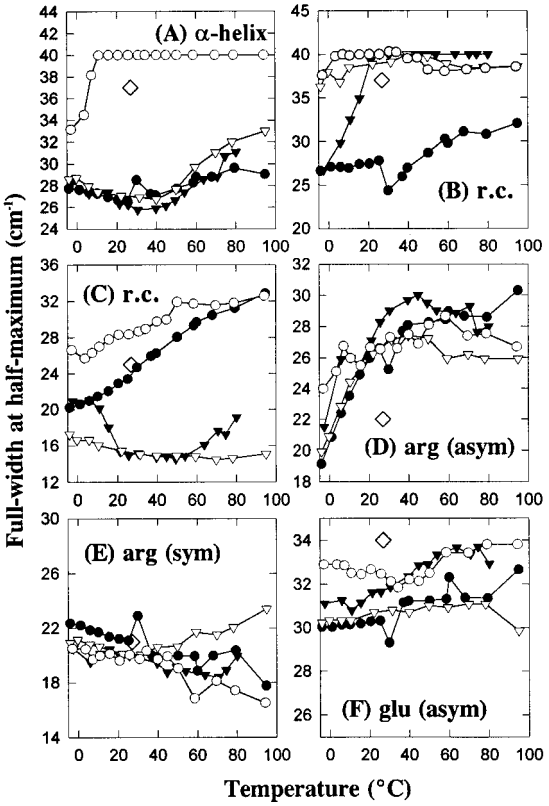

Figure 8. Full-width at half-maximum peak widths from the results of spectral fitting of all four peptides through the complete temperature range. (A)−(F) are the same as in Figures 6 and 7, as are the peptide symbol assignments. Units are cm^{-1}.

rising considerably up to about 25 or 30 °C and decreasing nearly back to its original value as the temperature is increased further. No consistent chain length trend is observable, although the $n = 1$ peak shows a slightly less sensitive response to temperature, with a shallow or nonexistent maximum. The room-temperature molar absorptivities of this Arg mode in the four peptides are about 20% higher than the value obtained from studies of Arg in solution (500 M^{-1} cm^{-1}).[17b] The intensity changes of the 1606 cm^{-1} mode, like the frequency changes, indicate a two-phase temperature response. The bandwidths also reflect the two-phase behavior of this mode with increasing temperature (Figure 8D). The width starts low, near 20 cm^{-1}, increases to about 27 cm^{-1} at about 30 or 40 °C, and does not deviate much from that value thereafter. The low-temperature behavior is consistent with the breaking of the hydrogen-bond and charge−charge associations which stabilize the helix. The high-temperature data indicate a different thermal response with presumably a different physical basis.

Intensity changes in the symmetric Arg mode, 1586 cm^{-1} in Figure 7E, decrease almost linearly for all peptides, with room-temperature values very close to that of the Arg residue in solution, 460 M^{-1} cm^{-1}.[17b] For the $n = 3$, 5, and 7 peptides, the responses are similar to that of the sister Arg mode (1606 cm^{-1}) in the high-temperature region.

In Figure 7F, the intensity of the asymmetric Glu peak near 1564 cm^{-1} is the least sensitive of all modes to temperature changes. As described above, the room-temperature intensity of this mode for each peptide was made to reflect the molar absorptivity,[17b] 830 M^{-1} cm^{-1}. Through the temperature range, intensities and bandwidths do not deviate greatly from their room-temperature value.

Physical Models for Interpreting Amide-I′ Intensity Changes. The relative intensities of the α-helical amide-I′ band can be used to calculate the percent helix of each peptide, and we can compare these values with those determined from CD measurements (data not shown).[7a] At 0 °C, assuming that the absorption intensity of the $n = 7$ peptide reflects that of a 90% helix (the value deduced for this peptide from CD), the calculated percent helicities of the other peptides are $n = 5$, 85%; $n = 3$, 74%; $n = 1$, 12%. These values are consistent with those assessed by their CD spectra, the IR values being 2%, 1%, and 11% greater than the CD values, respectively. When a similar calculation is performed at 90 °C, assuming that the intensity of the $n = 7$ peptide corresponds to 17% helix (again, the value obtained from CD), the calculated percent helicities of the other three peptides are $n = 5$, 16%; $n = 3$, 17.4%; $n = 1$, 0%. These values do not correlate well with the helical content predicted by the high-temperature CD measurements, the IR-predicted helicities being 31% and 45% greater than, and 99% less than, those values predicted by CD, respectively. This discrepancy led us to some interesting considerations.

In obtaining percent helicities from CD measurements,[12b] a mathematical model is used which relates the temperature-dependence of the measured ellipticity at 222 nm (the characteristic α-helix minimum) to the temperature-dependence of the number of amino acid residues in the chain *which are in helical conformation*. By measuring the first dependence, $[\Theta]_{222}(T)$, the second one can be calculated, $b_\alpha(T)$. Percent helicity is then obtained by ratioing the value of b_a at a given temperature to the total number of residues in the chain. Recall that in the normalization procedure for the amide-I′ IR intensities, the total number of amino acid residues was used for $b_{i,p}$ in eq 4. Thus, the molar absorptivities were calculated *per residue in the peptide*, and no attempt was made to relate temperature-dependent changes in infrared intensities to the temperature-dependent changes in the number of total amino acid residues *in helical conformation.* To analyze our intensity data in terms of chain length effects and the thermal unfolding of helices, we must distinguish two sources of temperature dependence. For the α-helix amide I′ mode, we rewrite eq 4 as follows

$$A_{\alpha,p}(T) = \epsilon_{\alpha,p}(T) * C_p * b_{\alpha,p} * (T) * l \qquad (5)$$

where $b_{\alpha,p}$ now refers to the *number of residues in α-helical conformation* for the pth peptide, and $\epsilon_{\alpha,p}$ is the temperature-dependent molar absorptivity of that peptide in units *per residue in α-helical conformation.* The number of peptide bonds in a random conformation is calculated

$$b_{\mathrm{rc},p}(T) = b_{\mathrm{total},p} - b_{\alpha,p}(T) \qquad (6)$$

where $b_{\mathrm{total},p}$ is the total number of residues in the pth peptide. These equations account for helical unwinding and the "concentrational" effect of that process on the different amide-I′ absorptions. In addressing specific questions of length dependence and unfolding mechanisms, we must determine values of $b(T)$ and $\epsilon(T)$ for the helical and random components in each of the peptides. Intensity changes due to $b(T)$ terms are "concentrational" and pertain directly to the mechanism of unfolding; intensity changes due to the $\epsilon_\alpha(T)$ and $\epsilon_{\mathrm{rc}}(T)$ terms arise from chain length and temperature effects at the level of the peptide bond itself.

Perturbation theory[20a] applied to the α helix provides a theoretical basis from which $b_{\alpha,p}(T)$ might be obtainable. As described above, perturbation theory uses dipole−dipole coupling to calculate the dependence of the helical amide-I′ vibrational frequency on the number of residues in the peptide; as the chain length increases, dipolar coupling increases and

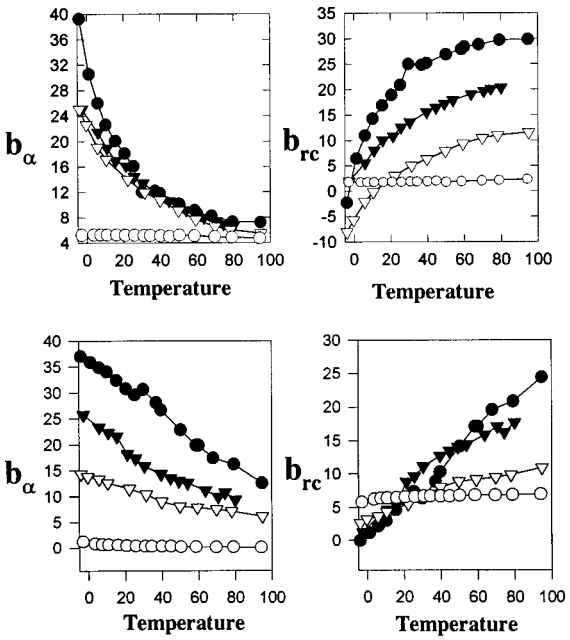

Figure 9. Temperature dependence of the number of peptide bonds in α-helical, b_α, and random coil, b_{rc}, conformation. (A, top) Derived from perturbation theory[21a] and the observed temperature-dependence of the 1630 cm^{-1} mode of the α-helix in Figure 6A. (B, bottom) Derived assuming a constant molar absorptivity $\epsilon_\alpha = 549$ M^{-1} cm^{-1} for all four peptides at all temperatures. Peptide symbols same as for previous figures.

the frequency decreases, asymptotically reaching a limiting value. The predicted theoretical dependence is shown graphically in Figure 8 of ref 20a. The data in that figure were approximated using an equation of the form $f = x/b$, where f is the frequency, b is the number of peptides in the helix, and $x = 98.2$ is a fitting parameter. Using this dependence of helical frequency on the number of contributing peptide bonds, $f(b)$, and combining it with the numerical dependence of the 1630 cm^{-1} helical frequency on temperature in Figure 6A, $f(T)$, we calculated the dependence of helical chain length on temperature, $b_\alpha(T)$ for each of the four peptides. The $b_{rc}(T)$ values were then calculated using eq 6. These values for $b_\alpha(T)$ and $b_{rc}(T)$ are plotted in Figure 9A.

The general trends in Figure 9A are consistent with thermally-induced helical unfolding, with reciprocal changes in the number of peptide bonds in helical and random conformations. However, there are some data points which are unreasonable. The largest possible values of $b_\alpha(T)$ or $b_{rc}(T)$ in the $n = 1$, 3, 5, and 7 peptides are 7, 17, 27, and 37, respectively, and the smallest possible value for each is 0. As seen in Figure 9A, for the $n = 7$ and $n = 3$ peptides in the low temperature range, our calculations overestimate the number of peptide bonds in the helix and correspondingly underestimate the number of peptide bonds in the random coil. After imposing the above maximum and minimum limits on the $b_\alpha(T)$ and $b_{rc}(T)$ values, eq 6 was used to calculate $\epsilon_\alpha(T)$ and $\epsilon_{rc}(T)$ for the helical and random coil modes in each of the peptide chains. These results are plotted in Figure 10.

Figure 10 indicates a significant molar absorptivity dependence on chain length for the α-helical dipoles. The calculated room-temperature values for $\epsilon_\alpha(T)$ are 40, 420, 620, and 1000 M^{-1} cm^{-1} for the $n = 1$, 3, 5, and 7 peptides, respectively. Recall that these values reflect the absorptivity of a single averaged single amide-I′ dipole, in α-helical conformation and in peptides of different lengths. The increasing values indicate a substantial increase in the local transition dipole of the amide I′ bond with increasing chain length. Interestingly, although the values are different for each of the peptide lengths, they do not show a significant temperature dependence. The local dipole appears to be sensitive to chain length (as far as distinguishing $n = 1$, 3, 5, and 7), but insensitive to whether the chain length around it is helical or disordered. Thus, in principle, the effect of the *presence* of other dipoles (chain length) can be distinguished from the effect of their specific *orientation* (thermal conformation).

These results are provocative but are in contrast to the results from studies on indefinitely-long peptides[17] in which room-temperature molar absorptivities for different helical types and lengths were found to have similar magnitudes. We believe that this model for calculating $b_\alpha(T)$, based on perturbation theory, does not provide satisfactory values and that the chain length and temperature dependencies determined for $\epsilon_\alpha(T)$ and $\epsilon_{rc}(T)$ are greatly affected by errors in the calculation of $b_\alpha(T)$.

Interpretation of intensity changes may also be approached by assuming that the molar absorptivities per residue, $\epsilon_\alpha(T)$ and $\epsilon_{rc}(T)$, are temperature and chain length independent. In this case, all absorption differences for different peptides at different temperatures merely reflect differences in b_α and b_{rc}; all absorption changes are concentrational in nature, resulting from a change in the number of peptide bonds contributing to each of the two distinct conformational states. For the helical mode, we initially assumed at all temperatures that $\epsilon_{\alpha,p}$ is equal to the room-temperature literature value,[17b] 460 M^{-1} cm^{-1}. (Recall that this value was obtained for indefinitely long peptide chains and calculated per residue; therefore, to the extent that the peptides in that study, chosen for their high helical content, were 100% helical at room temperature, this molar absorptivity would, in principle, be the same as our calculated value, in units *per residue in the* α*-helical conformation.*) However, use of the literature value overestimated the $b_{\alpha,p}$ values at low temperatures. The closest value of $\epsilon_{\alpha,p}$ which did not exceed the upper limit of $b_{\alpha,p}$ was 549 M^{-1} cm^{-1}. Using this number for all peptides at all temperatures, $b_{\alpha,p}(T)$ and $b_{rc,p}(T)$ were calculated. These values are plotted versus temperature in Figure 9B. The $b_{rc,p}(T)$ values give rise to $\epsilon_{rc,p}$ values for the 1650 cm^{-1} random mode which vary significantly as a function of temperature and chain length, between values of 120−5 M^{-1} cm^{-1} (data not shown; compare to literature value, 340 M^{-1} cm^{-1}).[17b] The data are thus not internally consistent with the assumption of constant molar absorptivities, indicating that the temperature dependence of ϵ_α, ϵ_{rc}, or both, have not been properly accounted for.

The $b(T)$ values plotted in Figure 9 (A and B) have different functional forms: while perturbation theory gave rise to an inverse dependence of bond number on temperature, the two-state model gave a sigmoidal dependence so shallow as to approach linearity. These two approaches appear to represent extremes in the calculation of molar absorptivity values, indicating either temperature/chain length dependence or independence, with the best interpretation probably lying somewhere between the two.

We carried out a third set of calculations of $b_{\alpha,p}(T)$ and $b_{rc,p}(T)$ using our $[\Theta]_{222}(T)$ values from CD measurements. These calculations gave rise to yet another set of $b_{\alpha,p}(T)$, $b_{rc,p}(T)$, $\epsilon_{\alpha,p}(T)$, and $\epsilon_{rc,p}(T)$ values (data not shown), similar to those in Figures 9A and 10, and again, showing internal inconsistencies.

Finally, in the determination of $b(T)$ and $\epsilon(T)$ values for modes arising from peptide secondary structure, one must consider the possibility that they are, in fact, not separable. The temperature and chain length dependence of the helical molar absorptivity may be fundamentally tied to the temperature and chain length

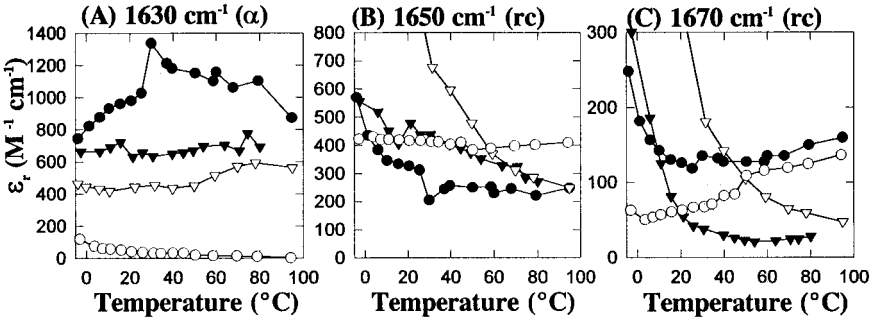

Figure 10. Temperature-dependence of amide I′ molar absorptivities calculated *per residue in each conformation*, calculated using $b_\alpha(T)$ and $b_{rc}(T)$ values from Figure 9A: (A) ϵ_α, for the 1630 cm^{-1} α-helical component and (B) and (C), ϵ_{rc} for the 1650 and 1670 cm^{-1} random coil components, respectively. Peptide symbols same as for previous figures. Molar absorptivities are in units of M^{-1} cm^{-1}.

dependence of the peptide conformation. This question appears to be outside the ability of the IR experiment to answer.

A stronger theoretical basis for the interpretation of vibrational intensity changes is clearly needed. It seems possible that, for the components of secondary structure, dipole−dipole perturbation effects should play a direct role in increasing or decreasing the absorption intensity, similar to the role suggested for frequency variations.[20a] To our knowledge, a reliable, quantitative model has not been developed to account for infrared absorption intensity changes in protein or peptide systems. Current normal mode calculations[21] for various biopolymers and analogues in various conditions may provide helpful results in future work in this area.

Mechanism for Helical Denaturation. Different spectroscopic probes naturally "see" different aspects of a system's secondary structure. It is not surprising that side-chain fluorescence gives rise to one picture,[22] perhaps "simple" in nature with a rather small number of parameters, while ^{13}C NMR gives rise to a picture which is much more complex and contains many more parameters.[3] Previous work[8a] using FT-IR to monitor helix unfolding of similar peptides suggested that amide-I′ intensity changes showed an isosbestic point between the helix and random components. In our data, what looks grossly to be an isosbestic point (Figure 1) between these two states, on closer examination and using the 2D technique for deconvolution, proves not to be. Our vibrational data indicate a model which is more complex than a simple two-state transition between a strictly helical and random coil conformation. The 2D correlation plots suggest strongly that the helical and random frequencies both vary significantly with the structural changes induced by temperature. Thus, although amide-I′ vibrations can be generally classified in terms of helical and random conformations, these two "states" are decidedly not static. As predicted by dipole−dipole coupling and perturbation theory, and as observed in the temperature-dependent frequencies, intensities and bandwidths in this work, each of these "states" is actually a dynamic collection of peptide bonds and possesses a unique dependence on temperature and secondary structural changes. While attempts were made to analyze intensity data in terms of the mechanism of helix unfolding, b_α, b_{rc}, ϵ_α, and ϵ_{rc} are highly correlated, and incorrect assumptions or errors in the calculation of one parameter drastically affect the other parameters and hence the conclusions drawn regarding structure.

Conclusions

We have demonstrated the usefulness of 2D analysis in the deconvolution and interpretation of FT-IR spectra which show changes in peptide secondary structure as a function of thermal denaturation. The utility of the 2D analysis has been illustrated, even when both frequency and intensity changes occur as a function of the perturbation.

The combination of curve-fitting with the 2D correlation analysis has resulted in a deconvolution of FT-IR spectral peaks through the −4 to 95 °C temperature range, elucidating the temperature-dependence of the vibrational parameters of the system. The infrared peaks are defined by three parameters, two of which are directly interpretable without the use of models or normalization procedures, namely peak position (vibrational frequency), and bandwidth. The results of our fitting procedure thus provide the first experimental observation of the effects of temperature and chain length on peak frequency and bandwidth for normal modes arising from both side-chain and backbone sources in the peptides. While the vibrational frequencies were observed to be relatively insensitive to chain length increases beyond approximately 15 residues, in agreement with perturbation theory,[20a] temperature increases caused significant shifts in the amide I′ frequencies. This indicates that at the vibrational level the helical and random coil "states" are dynamic structures with their own thermally-induced characteristics.

Interpretation of the third parameter, peak height (intensity), requires an accurate accounting of sample concentration and pathlength or else must rely on a proper normalization procedure using a known standard. For the peaks arising from the amide I′ modes, interpretation proves to be model dependent. We have constructed a framework for the interpretation and discussion of infrared absorption intensities for those normal modes arising from the secondary structural conformations of the peptide backbone. In addition to showing the information to be gained from quantitative infrared studies, the work here indicates some of the aspects which limit quantitative applications of infrared spectroscopy to problems in secondary structural studies of biopolymers.

Stellwagen's use of ^{13}C NMR to characterize the $n = 3$ helical peptide, Ac-W(EAAAR)$_3$A-NH_2, gave results[3] which distinguished end effects in thermal unfolding as well as suggested that the carbonyl terminal is stabilized less than the amino terminal. FT-IR data cannot provide information at the same level of molecular detail. Only to the extent that structural differences result in unique and distinguishable vibronic peaks can FT-IR be used to probe the more subtle levels of secondary structure. Subtle structural differences, such as end effects or

(21) (a) Krimm, S.; Bandekar, J. Vibrational Spectroscopy and Conformation of Peptides, Polypeptides, and Proteins. In *Advances in Protein Chemistry*; Anfinsen, C. B., Edsall, J. T., Richards, F. M., Eds.; Academic Press Inc.: 1986; Vol. 38. (b) Cheam, T. C.; Krimm, S. *J. Chem. Phys.* **1985,** *82(4),* 1631. (c) Mirkin, N. G.; Krimm, S. *J. Mol. Struct.* **1996**, *377(3),* 219.

(22) (a) Kiefhaber, T.; Schmid, F. X.; Willaert, K.; Engelborghs, Y.; Chaffotte, A. *Protein Science* **1992**, *1,* 1162. (b) Gryczynski, I.; Eftink, M.; Lakowicz, J. R. *Biochim. Biophys. Acta* **1988**, *954,* 244. (c) Thomson, J. A.; Shirley, B. A.; Grimsley, G. R.; Pace, C. N. *J. Biol. Chem.* **1989,** *264,* 11614. (d) Schmid, F. X.; Grafl, R.; Wrba, A.; Beintema, J. J. *Proc. Natl. Acad. Sci. U.S.A.* **1986**, *83,* 872.

the slightly different melting rates of the two terminal ends, appear to be lost in the statistical nature of the FT-IR data. A useful approach for increasing the resolution of IR data is the use of isotopic labels. Substitution of a ^{13}C with a ^{12}C in the amide group (carbonyl) decreases the amide I′ frequency by 35−45 cm^{-1}. This provides the ability[23] to vibronically distinguish the amide-I′ modes of one helical region from another. In this way, site-specific questions can be addressed, i.e., whether or not peptide bonds on the ends of the chain are mechanistically distinguishable from those peptide bonds in the center of the peptide. Projects of this sort, again based on interpretations using the 2D technique, are currently underway in our laboratory.

(23) (a) Haris, P. I.; Robillard, G. T.; van Dijk, A. A.; Chapman, D. *Biochemistry* **1992,** *31,* 6279. (b) Halverson, K. J.; Sucholeiki, I.; Ashburn, T. T.; Lansbury, P., Jr. *J. Am. Chem. Soc.* **1991,** *113,* 6701. (c) Tadesse, L.; Nazarbaghi, R.; Walters, L. *J. Am. Chem. Soc.* **1991,** *113,* 7036.

Acknowledgment. We heartily thank Dr. Richard Mendelsohn for suggesting that we pursue the 2D analysis and for other helpful discussions regarding this work and Dr. Dave Braddock for his help in the design of the thermostated cell holder and shuttle. We also thank Dr. Earle Stellwagen for his suggestions regarding the peptides to be used in these studies. This work was supported in part by GM34847. D.K.G. and B.P gratefully acknowledge the financial support of training Grants DK-07198 and HD07108, respectively.

JA970512M